

## FULL ARTICLE

# Optical plasticity of mammalian cells

Kaushikaram Subramanian<sup>1,2</sup>  | Heike Petzold<sup>1</sup> | Benjamin Seelbinder<sup>1,2</sup> |  
Lena Hersemann<sup>1,2</sup> | Ina Nüsslein<sup>1</sup> | Moritz Kreysing<sup>1,2,3\*</sup>

<sup>1</sup>Max Planck Institute of Molecular Cell Biology and Genetics, Dresden, Germany

<sup>2</sup>Center for Systems Biology Dresden, Dresden, Germany

<sup>3</sup>Cluster of Excellence, PoL | Physics of Life, Biotechnology Center of the TU Dresden, Dresden, Germany

**\*Correspondence**

Dr. Moritz Kreysing, Max Planck Institute of Molecular Cell Biology and Genetics, Dresden, Pfotenhauerstrasse 108, Dresden 01307, Germany.

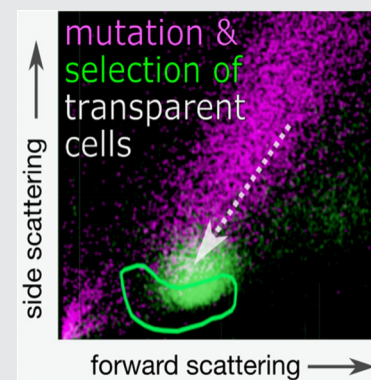
Email: kreysing@mpi-cbg.de

**Funding information**

Bundesministerium für Bildung und Forschung, Grant/Award Number: 031L0044; H2020 European Research Council, Grant/Award Number: 853619

**Abstract**

Transparency is widespread in nature, ranging from transparent insect wings to ocular tissues that enable you to read this text, and transparent marine vertebrates. And yet, cells and tissue models in biology are usually strongly light scattering and optically opaque, precluding deep optical microscopy. Here we describe the directed evolution of cultured mammalian cells toward increased transparency. We find that mutations greatly diversify the optical phenotype of Chinese Hamster Ovary cells, a cultured mammalian cell line. Furthermore, only three rounds of high-throughput optical selection and competitive growth are required to yield fit cells with greatly improved transparency. Based on 15 monoclonal cell lines derived from this directed evolution experiment, we find that the evolved transparency frequently goes along with a reduction of nuclear granularity and physiological shifts in gene expression profiles. In the future this optical plasticity of mammalian cells may facilitate genetic clearance of living tissues for in vivo microscopy.

**KEYWORDS**

biophotonics, light scattering, microscopy, nuclear architecture, optical clearing, photonics, tissue optics, tissue transparency

## 1 | INTRODUCTION

Since the advent of cell biology, light microscopy has been a key driver of biological discovery [1–3]. However, as modern biology is increasingly shifting toward the

detailed investigation of multicellular systems [4–7], a limitation for optical access is imposed by the opacity of most model tissues and model systems studied in the lab. Consequently, access by light microscopy is typically limited to the most superficial cells of a tissue.

Light–tissue interactions are wave-optically complex processes [8–10] with tissues displaying an immense variety of microscopic colloidal constituents, such as

Kaushikaram Subramanian, Heike Petzold and Benjamin Seelbinder contributed equally to this study.

This is an open access article under the terms of the Creative Commons Attribution License, which permits use, distribution and reproduction in any medium, provided the original work is properly cited.

© 2020 The Authors. *Journal of Biophotonics* published by Wiley-VCH GmbH.

membrane-bound and phase-separated organelles, membranes, and chromatin. These organelles are often in the size range of roughly a wavelength, rendering light scattering a complex biophysical phenomenon. For bulk materials, including tissues, to be transparent, it is essential to minimize internal refractive heterogeneities, such that light scattering becomes predominantly forward directed before the scattering ultimately disappears [10, 11]. Evolution has frequently found ways to generate tissue transparency. Examples include the cornea [12, 13], the retina [14–16], and many cases of whole-body transparency not only in insects [17, 18], but many deep-sea creatures, including vertebrates [9, 19–21].

We recently found that the mouse retina, a highly functional and cell dense tissue, achieves the highest transparency only during terminal stages of development and that this occurs through chromatin compaction that suppresses high-angle scattering [14, 15]. This study implicitly showed that genetics can be used to target the underlying molecular program [14]. Evidently, evolution demonstrates that tissues can be made transparent while conserving other biological functions. Physically, transparent tissues in nature owe their unique optical properties to a high scattering anisotropy factor  $g$  meaning, light that is scattered is deviated from the original path by only small angles (technically,  $g$  represents average cosine of the deflection angle of scattered light) [9]. Likewise, when fixed biological tissues are cleared for microscopy by refractive index matching techniques [22], the scattering anisotropy factor  $g$  is known to approach unity [23]. Hence, reducing light scattering of cells in a tissue is paramount for tissue transparency. The ability to manipulate the light scattering properties of live cells and there by the transparency of living tissues, would open up enormous potential for biological research.

As a first step toward the engineering of transparent tissues, we asked if the light scattering of optically non-specialized mammalian cells can be reduced while maintaining critical cell functions. To this end, we took a directed evolution approach to transform the optical properties of Chinese-hamster-ovary cells (CHO), a cultured mammalian cell line. We demonstrate that these mammalian cells possess a significant optical plasticity that allows the ratio of sideward versus forward scattering to be tuned as required for tissue transparency. We explore how the changed optical properties correlate with the changes induced in cell nuclear morphology and underlying changes in the transcriptional profiles of the evolved cells. We show that different states of increased transparency can be achieved without significantly reduced cellular fitness. We suggest that these results open exciting perspectives for the precision genetic clearing of living cells, tissues and possibly organoids.

## 2 | RESULTS

To drive the directed evolution of cellular transparency, we used a protocol comprised of multiple selection steps. First, random mutations were introduced in CHO cells by transfecting a plasmid containing an antibiotic resistance cassette followed by antibiotic selection. The plasmid also harbored a crystallin gene (*Cry $\beta$ a2*), which is involved in maintaining the transparent state of the rodent lens and which we initially thought could potentially also improve optical properties of our cells [24–26]. Using this standard non-targeted transfection, the plasmid is expected to integrate randomly in the genome. It is expected that the expression of the antibiotic resistance gene in the presence of the antibiotic drug (Neomycin) leads to the selection of cells that have the plasmid stably integrated into their genome.

Importantly, integration into the genome might impact the optical phenotype of the cells in two different ways. Either (a) via the ectopic expression of the introduced crystallin gene or (b) nonspecific changes in the expression levels of endogenous genes. The latter ones are known to result as side effects caused by mutations that may be induced upon plasmid transfection. While non-specific, such off-target effects are frequently found to facilitate directed evolution in the lab. After stable integration of the plasmid in the genome of CHO cells, we quantified their optical scattering by FACS (Figure 1). To our surprise, we found that stably transfected cells had a greatly diversified optical phenotype, with most cells scattering greater amounts of light than the original wildtype (WT) cells (Figure 1A). At the same time, we noticed that the amount of debris in the medium increased significantly (lower left corner), likely reflecting residuals from dead or stressed cells.

### 2.1 | Selection of cells with reduced light-scattering signal

After selection of cells based on antibiotic resistance, we used the sorting capabilities of FACS to impose an optical selection pressure to drive the seemingly diversified population of cells toward a state of reduced light scattering, in particular reduced large-angle scattering which is required for tissues to become transparent according to the Henyey Greenstein (HG) model (Figure 1B) [27, 28] as classic way of approximating light scattering in tissues.

Specifically this reduction of large angle scattering results in a more forward directed light scattering distribution, experimentally measured as the ratio of

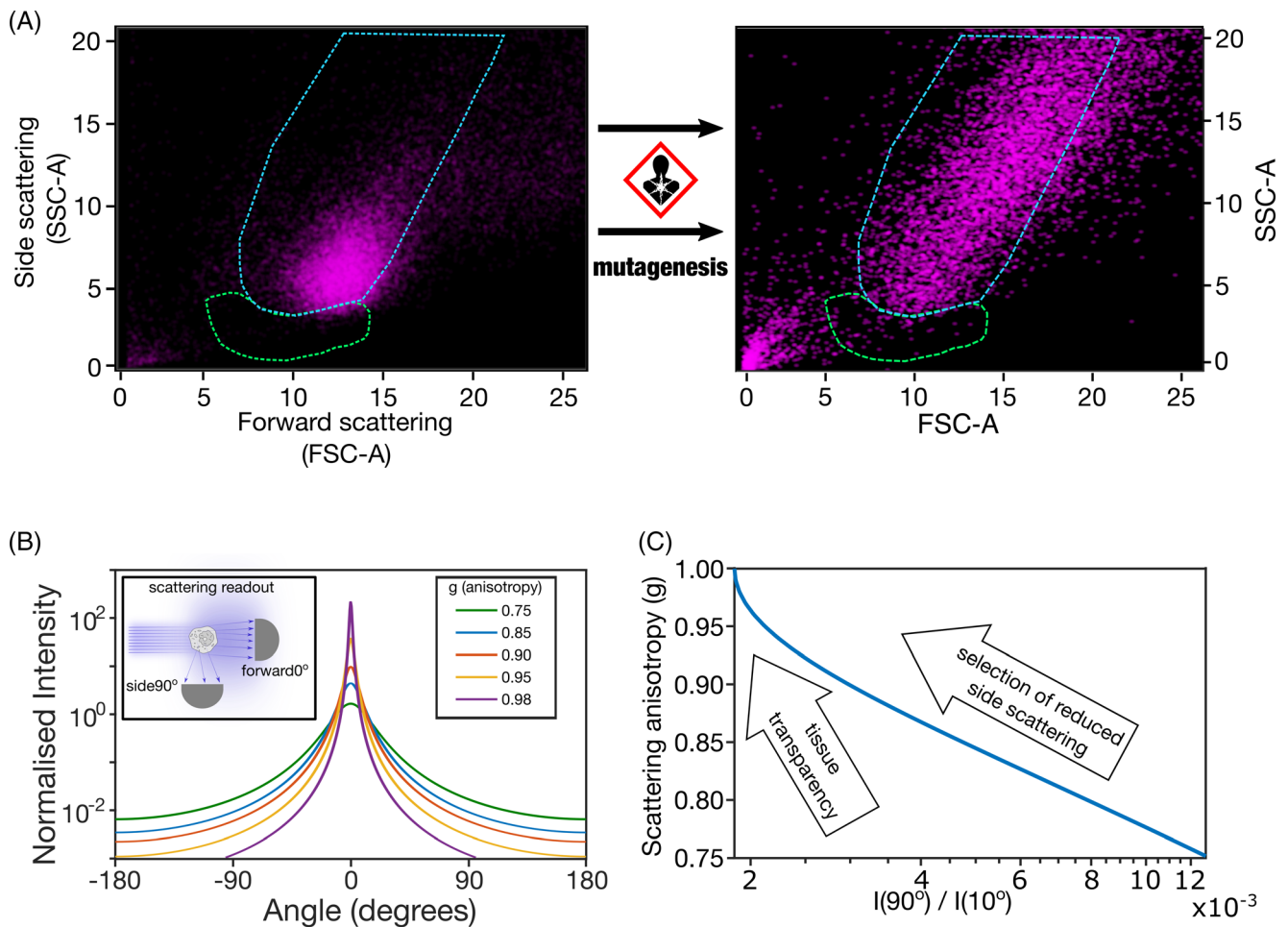


**FIGURE 1** Mutagenesis by plasmid integration diversifies optical phenotypes of suspended mammalian cells. A, Random integration of a plasmid in the genome leads to strongly diversified phenotypes in a polyclonal population of transfected mammalian cells (Chinese hamster ovary cells, CHO). Both integrated forward and side scattering (forward/side-scattering-area, FSC-A, SSC-A) distributions widened greatly, with a general tendency toward increased light scattering. B, Henyey-Greenstein distribution as a classic model of light scattering by tissue. Transparent tissues, including clear tissues typically have an anisotropy factor “g”, which weights forward and sideways scattering, close to unity. (Inset) Simplified schematic of optical readout scheme to quantify forward and sideward light scattering in a fluorescence-assisted cell sorter (FACS), collected under 10 and 90 degrees scattering angles, respectively. C, Anisotropy factor g as a function of differential light scattering signals at 90 and 10 degrees

scattered light intensities at  $I(90^\circ)$  and  $I(10^\circ)$ . With a decreasing ratio of these intensities, the HG model of light scattering, predicts a monotonous increase of the anisotropy factor (‘g’, Figure 1C), a key determinant of tissue transparency. For our experiments, we selected the approximately 1% least side-scattering cells (side-scattering area, SSC-A, green gate in Figure 2), practically isolating approximately 10 000 cells with strongly reduced side-scattering signal.

Next, we cultured this low-scattering fraction of cells and observed their robust replication at a rate roughly comparable to WT, meaning that after 10 days of growth a highly diluted population reached confluency again. During these approximately 10 doublings, the likely heterogenous initial population of cells was inevitably selected based on replicative fitness. In this period,

the abundance of cells with a 50% prolonged cell-cycle time would be reduced as much as  $2^{(10\text{days}/1\text{day})}/2^{(10\text{days}/1.5\text{day})} = 10.1$ -fold compared to WT cells. We observed that cells were still able to spread on glass and showed no striking abnormalities (see subsequent sections for more detailed analysis of the phenotype). The cycle of optical selection and replication was repeated for a total of three rounds (compare Figure 2). FACS analysis showed that the side scattering of optically selected cells was significantly reduced compared to non-transfected cells (Figure 2 lower branch). This improvement of optical properties on the population level closely reflects the selection pressure. At the same time, transfected cells that were gated according to a high scattering signal transformed to match this alternative selection pressure (Figure 2, blue upper gate). Importantly, non-transfected

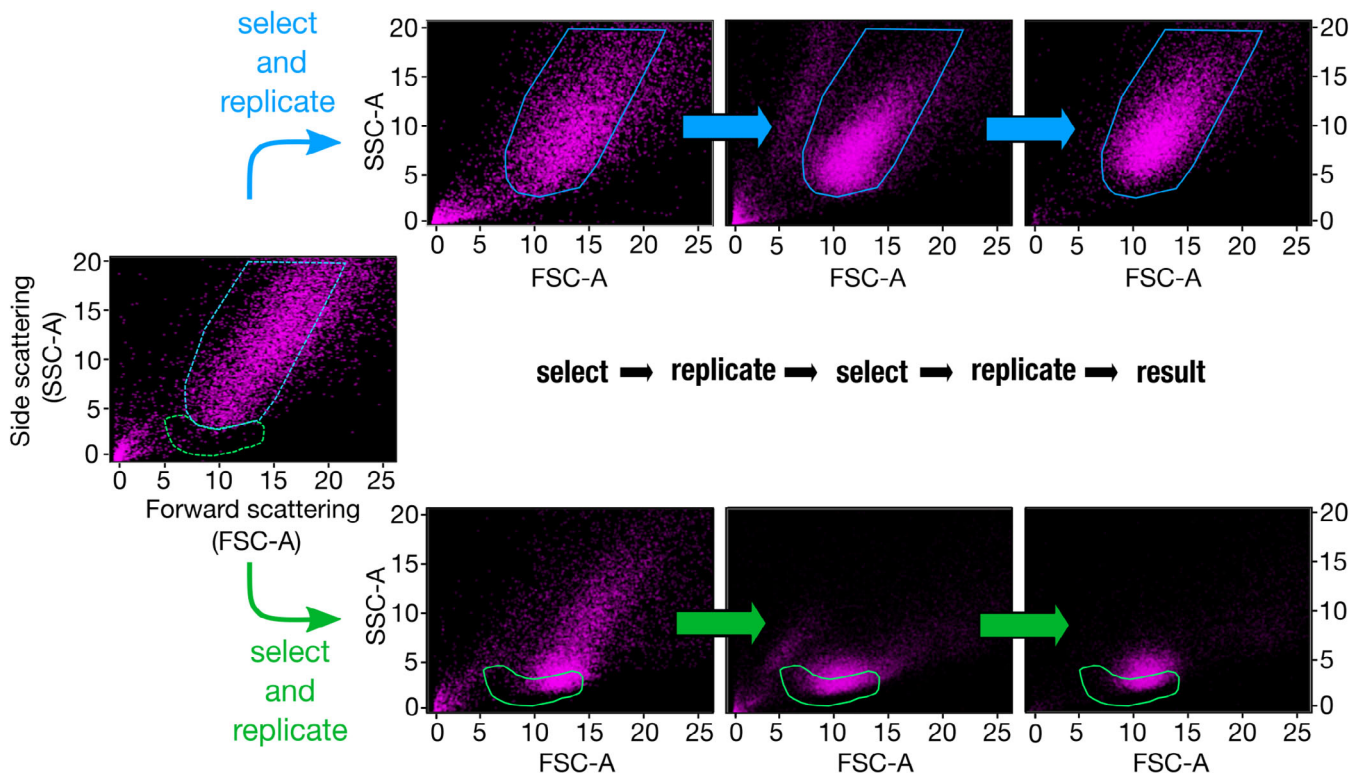


**FIGURE 2** Optical selection and re-culturing of mutated cells. After mutagenesis (see Figure 1), the stably transfected cells were sorted according to optical properties, namely integrated forward and side scattering signals (FSC-A, SSC-A). Cells were sorted from a low-scattering (green) and a high-scattering gate (blue). After 3 rounds of sorting and replication, the heterogenous population transformed under the optical selection pressure, yielding cells that displayed elevated (upper branch) or significantly reduced (lower branch) light-scattering characteristics

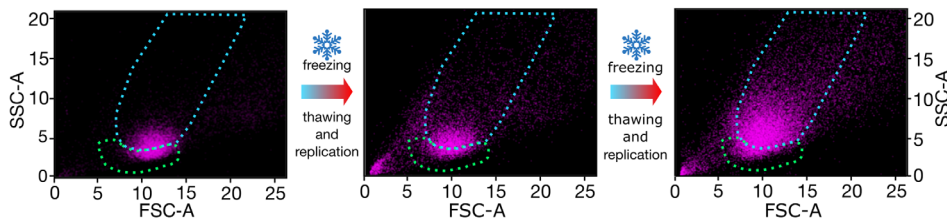


**FIGURE 3** Exposure to stress eliminates cells with reduced fitness. Exposure of low-scattering cells to freeze–thaw and expansion cycles lowers the abundance of non-fit cells. This process also counter-selected many, but not all, low-scattering cells

control cells that were optically selected did not retain their low scattering properties (Figure S1). These control experiments emphasized that the optical selection, rather than nonspecific factors or instrument drift, caused the reduction in light scattering for the cells of interest. Even though non-transfected cell lines show a significant spread in light-scattering signals, which is likely governed by varying cell positions and orientation with respect to the laser beam [29, 30], the high throughput of FACS is suitable to quantify and enrich cells with modulated optical properties. To summarize our directed evolution experiment, we were able to generate replicating cells with reduced light-scattering properties in only three rounds of optical selection.

## 2.2 | Cellular fitness of optically selected cells

To assess how fit the optically improved cells were, we exposed cells to severe stress in the form of freeze–thaw cycles, spaced by 7 to 10 days of recovery and population expansion. While doing so, we realized that the evolved heterogenous population of low-scattering cells started to scatter more light again, despite significant time allowed to recover from freezing (Figure 3). These experiments show that (a) the evolved population of low-scattering cells partially maintained the ability to cope with severe stress and recover after freezing; (b) the population was likely heterogenous, with the most transparent cells

possessing a lower ability to survive in the presence of stress, which would explain the upshift in scattering; and (c) a small but significant fraction of recovering cells still possessed a low-scattering state (compare Figure 3, green gate right panel).

### 2.3 | No effect of crystallin overexpression on cell transparency

As discussed before, the observed changes in optical properties of CHO cells could be either due to

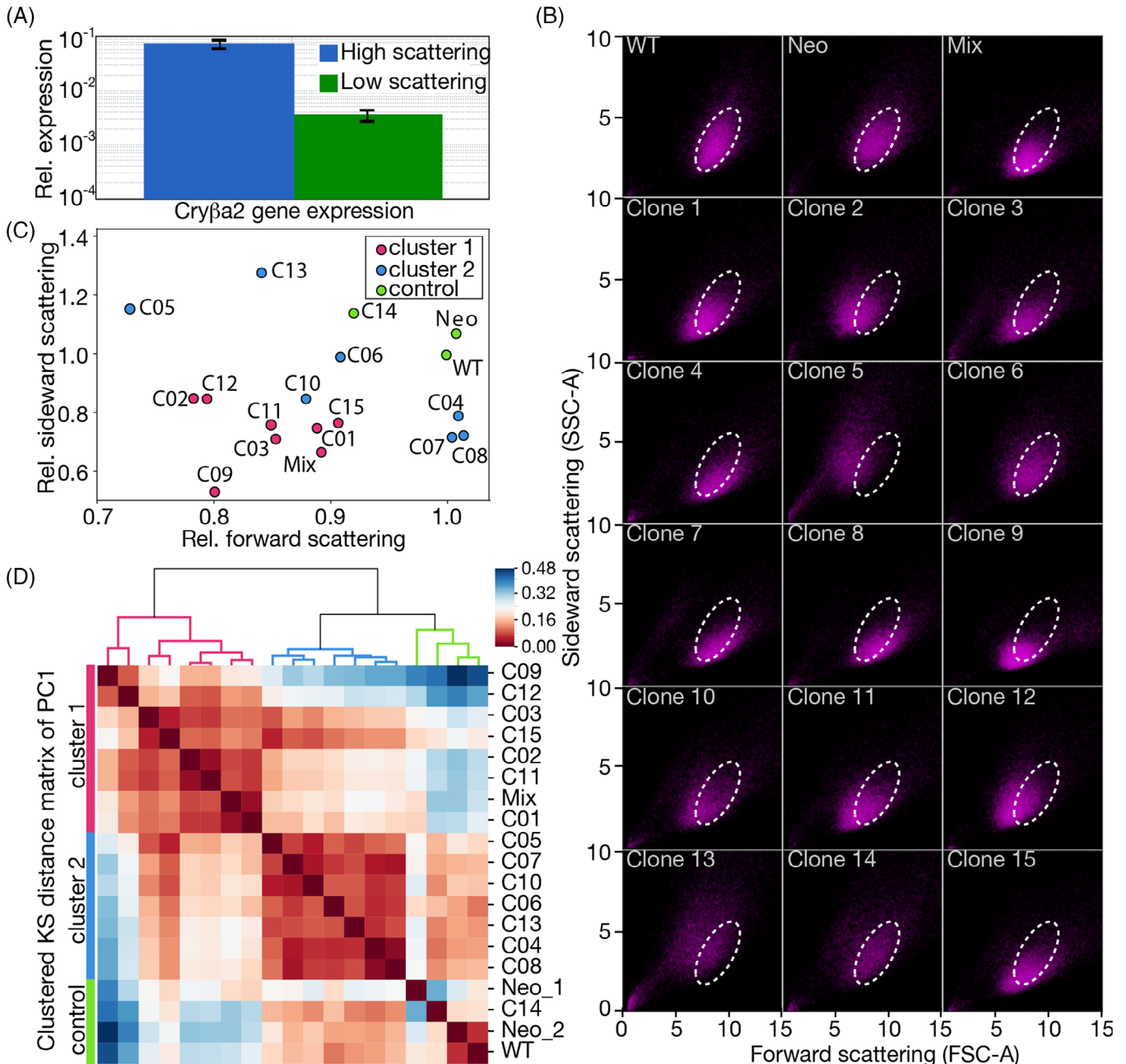


**FIGURE 4** Light scattering from sub-population and monoclonal cell populations. A, Transparency is not cause by crystallin expression: quantitative molecular analysis reveals higher crystallin expression in cells with high light scattering. B, Light scattering signals in a forward and sideward direction for 15 isolated monoclonal cell lines measured by FACS, (typically >50 000 cells). The white oval represents a visual guide illustrating the shape and distribution of light scattering by various clones compared to the WT population. C, Cell lines show distinct centers of mass, with 12 of 15 showing reduced forward scattering and 11 of 15 cell lines showing reduced sideward scattering. The coloring is based on the three major clusters identified in, D. D, Hierarchical clustering of cumulative distance of first principal component for scattering signals (area = integrated signal, height = peak signal, width = duration of signal) each for forward and sideward scattering direction

(a) overexpression of the crystallin gene *Cryba2* (b) or altered expression of endogenous genes due to the disruptive effects of the integration. To investigate the extent to which crystallin overexpression is related to improvements in cell transparency, we compared *Cryba2* mRNA levels in high- and low-scattering fractions. Notably, we found stronger crystallin expression in cells that scatter greater amounts of light (Figure 4A). This suggested that the reduction of light scattering in selected cells cannot be explained by the overexpression of *Cryba2* gene, but rather through the acquisition of mutations which are likely to cause more complex changes in the expression of endogenous genes (as later we confirmed by mRNA sequencing, read below). In support of this view, attempts to use our directed evolution scheme had reduced success with MDCKII cells, which possess redundant copies of most genes (Figure S2). Such a genetically induced shift in the endogenous gene expression profiles would further explain a strong optical heterogeneity in the pool of evolved cells.

## 2.4 | Distinct monoclonal colonies of transparent cells

To gain an understanding of the optical diversity of low-scattering-cells, we derived single monoclonal colonies from individual cells, which were still measured with a low scattering signal after freeze–thaw cycles. We found that 15 out of 24 picked single cells recovered and successfully expanded to full populations, and all 15 of these colonies were then found to be sufficiently fit to reliably survive another freeze–thaw cycle. After several rounds of expansion, cells were characterized again in terms of their light-scattering properties. These experiments confirmed reduced side scattering in 12 out of 15 cell lines, and 11 out of 15 isolated cell lines showed reduced light scattering in a forward direction when compared to original WT or control cells transfected with a vector containing the antibiotic (Neomycin) resistance gene but that had not been exposed to optical selection (Figure 4B, C). Owing to the multidimensional nature of the FACS data, principal component analysis was used to reduce dimensionality from the initial 6 optical parameters (area, width, and height of the signal) measured for FSC and SSC, respectively, to a 3-parameter space. The PCA shows that about 71% of the variance is captured in the 1st component. However, the factor loadings or the correlation of the PC1 with the raw data is such that all the 6 measured parameters contribute to the generation of the PC1 with similar significance range (30%–49%). The distribution of the 1st principal component scores was then used to determine the distinction between

populations using the K-S test metric [31, 32]. This metric suggests that all of the clonal populations are statistically different from WT and controls and also among themselves (Table S1). However, the evolved cells do occupy different phenotypic niches with the monoclonal cell lines forming 2 distinct clusters different from the WT and control cluster (Figure 4D), a finding not easily accessible just by visualizing the light scattering in 2-dimensional space. These data suggest that CHO cells, a mammalian cell line, have a significant optical plasticity that allows modulation of optical properties towards higher scattering states as well as more transparent ones. Forward and sideward scattering seems largely uncorrelated across populations (Figure 4C), indicating that changes in optical properties occurred during directed evolution and are unlikely to be explained by the variation of a single parameter. More systematic analysis of this optical data suggests that cell lines fall into two to three clusters that differ from WT (Figure 4D).

## 2.5 | Cellular phenotypes and reduced nuclear substructure

Next, we asked if one can identify relationships between reduced light scattering and the cellular phenotype, and if the aspects of scattering reduction could be mechanistically understood by changes in cellular organization. As a large fraction of the cell is occupied by the nucleus, which is known to contribute significantly to light scattering [14, 15, 33–35], we probed for correlations between extreme scattering phenotypes (compare Figure 4C) and nuclear morphology. For this we used 3D spinning-disc volumetric microscopy to analyze features of spatial chromatin distribution in nuclei of Hoechst-stained CHO cells (Figure 5A). Nuclear areas were significantly decreased for clones C05, C08, and C13 compared to both WT and Neomycin control cells (Neo, Figure 5B). However, nuclear size remained about the same for C09, which showed low scattering in both forward and sideward directions compared to controls. This shows that reduced scattering can be independent of size. However, C09 showed lower granularity (relative amount of edges and chromatin compaction parameter, CCP, see supplementary information for details [Appendix S1]) compared to controls and the high side-scattering colony C13 (Figure 5C,D). To look for a systematic relationship between scattering and these variables across cell lines, we performed linear correlation analysis between nuclear features and scattering behavior with the inclusion of two more colonies (C11 and C15) with (improved) average scattering properties (Figure 5E). We observed that granularity showed a distinct correlation with side

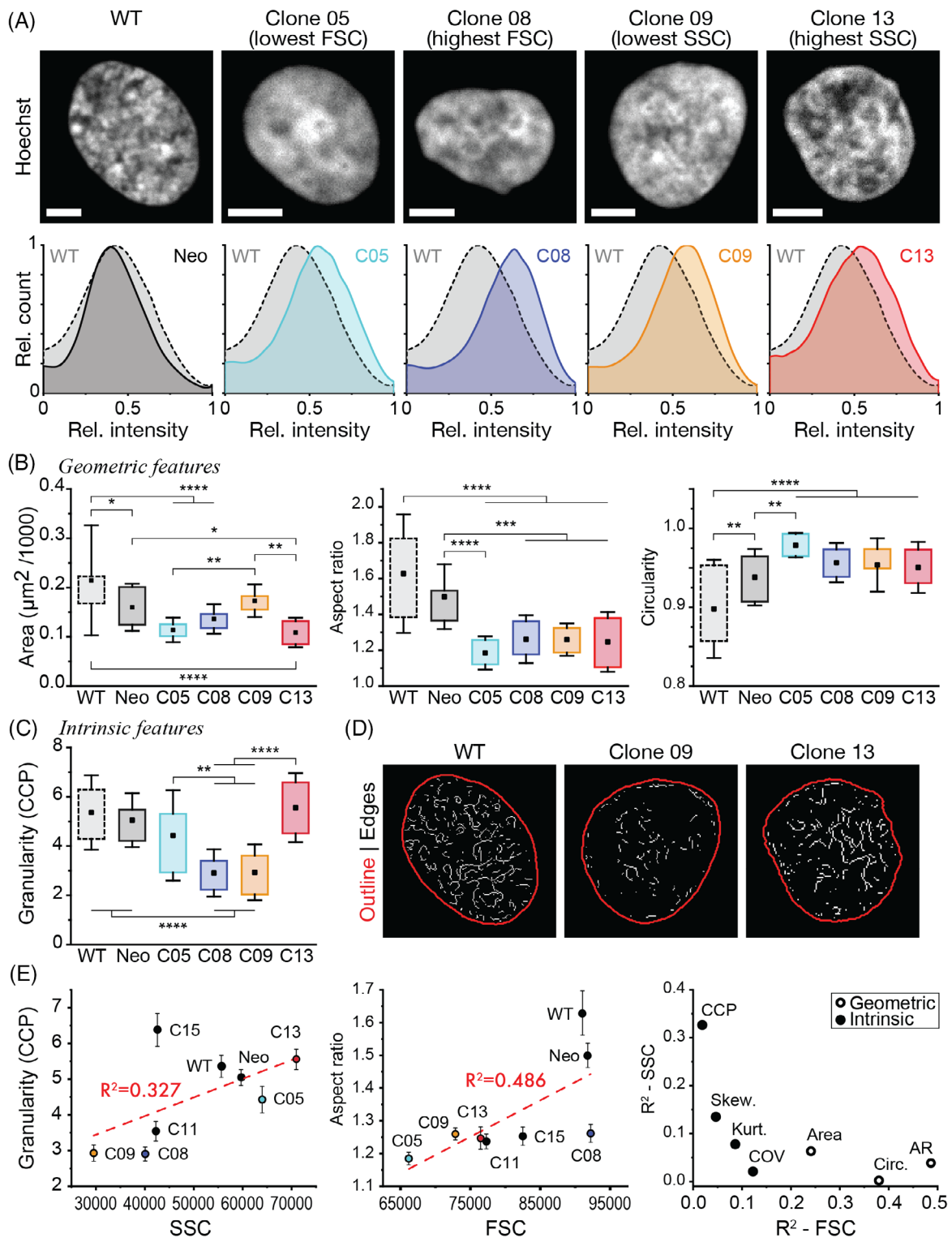


**FIGURE 5** Transparent cells show reduced nuclear sub-structure in confocal light microscopy. A, Nuclear phenotypes of 4 selected CHO clones with extreme scattering properties, along with the histogram of the Hoechst fluorescence signal as a reporter for DNA density ( $n = 23$  nuclei per condition). B and C, Geometric features of nuclei and intrinsic properties of chromatin distribution. D, Examples of nuclear segmentation and feature detection. E, Linear correlation of nuclear phenotype features with side and forward light scattering (SSC, FSC) as obtained from FACS analysis. Granularity of chromatin (CCP) showed the strongest correlation with side-scattering behavior, while forward scattering was most strongly correlated with aspect ratio. Scale bar in panel A is  $5 \mu\text{m}$

scattering ( $R^2 = 0.33$ ) but not forward scattering ( $R^2 = 0.02$ ). It is well established that side scattering is related to high cell or nuclear granularity and can be used to discriminate different cell types, while no stringent reliable relationship has been established for forward scattering [32]. In our analysis, both nuclear aspect ratio and circularity revealed a correlation with forward scattering ( $R^2 = 0.49$ ,  $R^2 = 0.38$ ). Generally, intrinsic features appeared to explain changes in side scattering, while geometric features were more predictive of forward scattering. In conclusion, our data confirm that the nucleus is a large contributor to cellular light-scattering behavior. Even though we expect scattering properties to be multifactorial, some nuclear features showed relatively high explanatory power with regard to light scattering, with side scattering being particularly correlated with measures of intrinsic chromatin organization.

## 2.6 | Altered endogenous gene expression profiles within physiological boundaries

Next, we asked if the evolved transparent cells display different gene expression profiles, and if so, whether these could be seen as physiological. For this, we purified messenger RNA from the total of 15 cell lines (mixed population, 12 monoclonal cell lines derived from it, WT and control) and determined its content via Illumina sequencing. To start with, the bioinformatic analysis excluded the possibility of a change in optical phenotype due to foreign cell contaminations that could have been picked up during the sorting process (Figure S3). More interestingly, we found that optical selection favored cells with plasmids integrated in genome positions where they are highly transcribed. This affect the transcription of the antibiotic resistance. At the same time, the RNA sequencing confirmed the earlier preliminary result obtained by PCR showing that induced transparency cannot be explained by overexpression of the crystallin gene. Specifically, we found cells only to express part of the crystallin and the expression levels correlated very weakly with light scattering. Quantitative analysis of the putative genotype phenotype relationship suggests that only 4% and 6% of forward and sideward scattering respectively may be explained by crystallin overexpression (Figure S4). We therefore followed up on the hypothesis that the transparency of our evolved cells is determined by complex changes in their transcription profiles.

When analyzing the transcription profiles, we found that the mixed population of transparent cells contained 1254 differentially expressed genes, with 566 genes upregulated and 688 genes downregulated in comparison

to the WT. We then asked if the isolated monoclonal cell lines were transcriptionally distinct from the WT and control cells. For this, we repeated the sequencing and classified the transcript-level data by automatic cluster analysis. As a result, we found that evolved cells clustered into transcriptionally distinct groups (Figure 6A). In particular, we observed a distinct group containing WT and control cell lines, one clearly distinct group containing the repeatedly sequenced heterogenous population of transparent cells prior to single cell isolation, and two slightly more weakly defined groups from monoclonal cell lines. A similar grouping can also be observed in a cluster diagram considering the first two principle components of variability in the underlying transcriptional data (Figure 6B). Here, evolved transparent cell lines also fall into groups that are transcriptionally separated from the distinct WT and control groups, the latter two being found in closest proximity.

When focusing on the common differences in the gene-expression profiles of the low-scattering clones versus the control cells (WT and neomycin control), we found that 198 genes were at least 2-fold differentially expressed in the evolved cells (124 downregulated and 74 upregulated, adjusted  $P < .01$ ). Gene enrichment analysis based on hamster orthologues of human genes (Figure 6C) further revealed that the genes differentially expressed in the low-scattering clones broadly affect the extra cellular matrix (ECM) organization and its constituents. Potentially, the changes in ECM organization may explain the observed changes in cell morphology and granularity through cellular and nuclear mechanosensitive feedback mechanisms [36–38]. In support of this view, the same analysis also revealed receptor tyrosine kinases to be affected, an important class of molecules involved in transmitting extracellular signals into the cell, and via integrin-dependent pathways all the way to the nucleus [39, 40]. Furthermore, collagenous structures have been shown to play a key role in tissue transparency [13, 41]. While we do not see evidence of highly regular collagen assemblies, one possibility is that we activated pathways of cellular transparency that happen to be coregulated with collagen-dependent pathways responsible for the transparency of ocular tissues.

More generally, 4 out of 6 cell lines that form transcription cluster 1 (Figure 6A) were previously also clustered together regarding their light-scattering phenotype (Figure 4D), indicating potentially underlying genotype-phenotype relationships, where a common genetic pathway or mechanism could lead to similar optical phenotypic characteristics. Correspondingly, for transcription cluster 2, we even found that 5 out of 6 cell lines previously showed similar light-scattering characteristics. No sequencing data was obtained for the remaining 3 cell

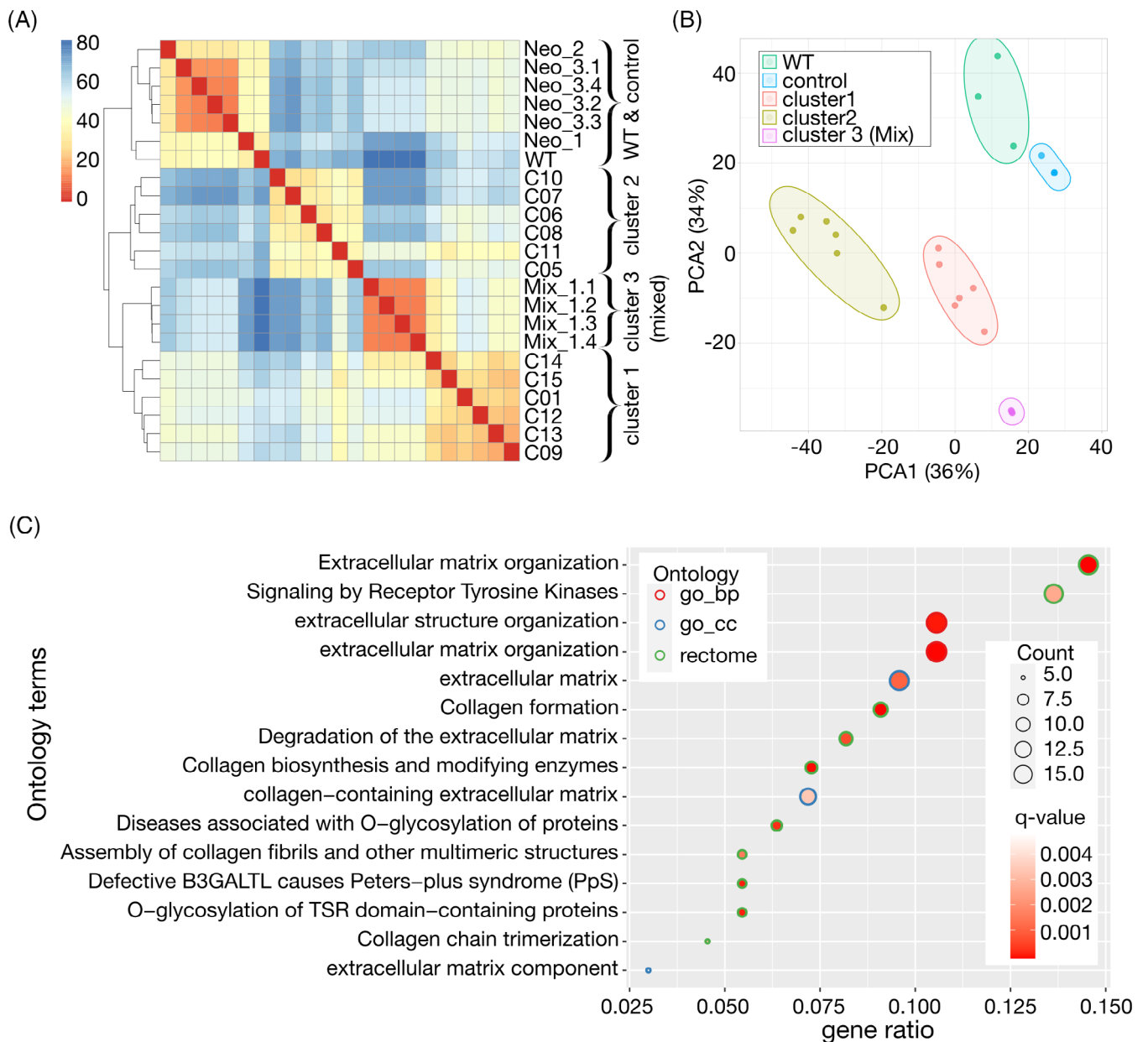


**FIGURE 6** Transparent cells are genetically distinct from the original cells. A, Transparent cells cluster into groups that are genetically distinct from WT and control cells and feature hundreds of differentially expressed genes (automated HC clustering [before PCA] with ward D2 distance metric). B, Principle component analysis of gene expression profiles shows relative positioning of the transparent cell clusters 1 and 2, and the initial heterogeneous population (Mix) with respect to the WT and control cells. C, Gene ontology of the differentially expressed genes in the evolved low scattering cells vs the WT and control cells. All the clones were pooled and compared against the WT and control for the gene enrichment analysis

lines. Beyond these clear trends, exceptions were found. Cell lines 9 and 13 are closely related in terms of transcription profiles despite having very different nuclear granularity and sideward light-scattering characteristics. Similarly, clones 5 and 8, which are in the extremes of the forward scattering, seem to cluster together transcriptionally. These observations might reflect that light scattering by cells is multifactorial, and one possibility could be that after an early selection of a low-scattering cell

line, subsequent mutations occurred to increase the light scattering of cell line 5 and 13.

Next, we asked if the transcriptome data reveals details about the physiological state of the cells. Out of 25 072 annotated hamster genes, 12 597 passed the applied filter of at least 10 counts in any of the clones were considered for differential gene expression analysis. 10 008 of these genes were found to have high confidence one-to-one orthologues in Humans with 2334 genes that

are annotated with the GO term “response\_to\_stress” (GO 0006950) or any child term (Figure S5). From the list of 198 differentially expressed genes, 174 were found to have human-hamster one-to-one orthologous with 38 genes annotated with the GO term “response to stress” (GO:0006950) or any child term (Figure S6). None of these GO terms came up as significantly enriched (Figure 6C). Moreover, heat shock proteins their key regulator *hsf1* also were only weakly modulated and revealed no significant difference between transparent and control cells.

Furthermore, we looked at the gene expression levels of housekeeping genes that cells require for essential processes (Figure S7). Here, we also found them to be at normal expression levels in each of the transparent cell cluster 1 and cluster 2 compared to WT and control group. In summary, our data does not show elevated levels of cellular stress and supports the view of a normal physiological state in the evolved cells. From this, we conclude that CHO cells, a mammalian cell line, have a significant optical plasticity that enables modulation of optical properties toward higher scattering states as well as more transparent ones, via complex gene expression shifts that are compatible with the maintenance of cellular functions.

### 3 | DISCUSSION

We found that cultured CHO cells, a model mammalian cell line, possess a significant optical plasticity. Cells can be guided to drastically change their optical phenotype, which is associated with significant changes in transcriptional profiles. These changes are uncorrelated with the crystallin expression level and are more likely a result of unspecific, random, mutagenic effects of the plasmid integrating into the genomes. Whereas most of the mutations that we initially induced increased scattering, we managed to select cells that showed significantly reduced light scattering, particularly light scattering at large angles and were also able to replicate and withstand high stress. Strikingly, this reduction in scattering was frequently observed alongside a reduction in nuclear substructure (an established determinant for light scattering) [14, 23, 33–35, 42].

The attempted approach to modulating and matching the refractive index of the intracellular space may be non-trivial because of the wide range (1.33–1.40) of refractive indices of the various important cellular organelles [43, 44]. Refractive index matching in the lens requires both high concentrations of crystallin without precipitation or aggregations, which might not be achievable by the overexpression of a single crystallin, as well as the dissolution

of cellular organelles. Even though, the light scattering and protein content of a cell is predicted to initially increase and peak at a volume fraction of 13% and later decrease [45], with the typical protein concentration in a cell of up to 20% to 30% [46] the increase in light scattering upon crystallin expression might reflect the precipitation, or aggregation of solubilized proteins [47]. As occurs in attempts to modulate intracellular refractive index by injection of biologically compatible matching agents, such as glycerol [42], the forceful overexpression of proteins might also have unexpected effects on the physical properties of the cytoplasm and potentially on the spatial organization of the cell.

Directed evolution is an extremely powerful way to produce phenotypes that comply with selection criteria, and we identified a suitable pipeline to harness the potential of high-throughput methodologies. Nevertheless, one may ask why cells that were never meant to be transparent show the ability to modulate their optical appearance towards a transparent state. We see three reasons for this. First, scattering of light by cellular constituents is a complex wave-optical phenomenon that is non-linearly impacted by (a) size range and (b) refractive index contrast, and is (c) susceptible to spacing and to a lesser degree shape [9, 45]. Changing any property will likely change scattering amplitudes. Second, mammalian cells are known to owe their robustness to the redundancy of functional pathways that may even compensate for the loss of entire chromosomes. Gradually exchanging primary pathways for redundant ones constitutes degrees of freedom that impact determinants of transparency without compromising cell fitness, or where fitness is impacted, competitive growth eliminates non-physiological responses. Third, different cell types of the same organisms are known to exhibit a range of optical properties, even much wider than explored here [10]. In parts, the phenotype of reduced nuclear substructure is reminiscent of rod cells in the mouse retina [14, 15] where granularity is also reduced, albeit by the central compaction of heterochromatin to a giant chromocenter. Lastly, nuclear granules also disappear in the lens, and reduced light scattering is the central characteristic of transparent animals in the deep sea [9].

### 4 | OUTLOOK

We predict that systematic screening of transcriptomes over many optically evolved cell lines will enable the genomic basis of optical plasticity to be dissected in mammalian cells. As the genetic basis of optical plasticity begins to be understood, and as individual molecular regulators sufficient to modulate cellular light scattering are

identified by screening, it might become possible to use precision gene editing strategies [48] to increase the transparency of cultured cells, primary cells, progenitor cells, and specific tissues in living organisms [49], and also large organoid structures. Genetically cleared living tissues could either be directly studied by light microscopy or provide a transparent window onto underlying tissues of interest. Furthermore, we suggest that the optical properties of cells could be evolved in the presence of other selection pressures that would guarantee the stability of central pathways in the context of interest. In previous years, scattering reduction made tissues transparent for microscopy [50]. With genetically enhanced, optically superior tissues, the potential of a wide range of microscopy techniques might no longer be restricted to the surface and instead allow imaging deep inside living tissues.

In conclusion, we have shown in a cultured mammalian cell line, that living biological cells can display significant optical plasticity. Microscope optics have been tweaked to perfection in recent decades, such that in many cases the sample itself is now the optical bottleneck. We therefore suggest genetic engineering of the optics of the sample as a promising approach to achieving unprecedentedly clear views deep into living tissues and organisms.

## ACKNOWLEDGMENTS

We would like to acknowledge discussion with Elisabeth Knust, Jamie Blundell, Iain Patten, Anne Grapin-Botton, and Jochen Guck for helpful discussions and comments. We would like to acknowledge help from the TU Dresden Sequencing facility, especially Andres Dahl, and Silke Winkler, help from the MPI-CBG Scientific computing facility, especially Ian Henry, as well as the MPI-CBG FACS facility, Marc Bickle and Mihail Sarov from the MPI-CBG screening and transcriptomics facilities. Open access funding enabled and organized by Projekt DEAL.

## CONFLICTS OF INTEREST

The authors declare no potential conflict of interest.

## AUTHOR CONTRIBUTIONS

Heike Petzold and Moritz Kreysing designed directed evolution experiments which Heike Petzold carried out. Heike Petzold and Ina Nüsslein carried out optical selection experiments. Kaushikaram Subramanian, Heike Petzold, and Moritz Kreysing planned RNA sequencing experiments, which Kaushikaram Subramanian and Moritz Kreysing interpreted. Lena Hersemann performed the bioinformatics analysis of the sequencing data. Benjamin Seelbinder and Kaushikaram Subramanian performed fluorescent microscopy of cell nuclei and Benjamin Seelbinder

performed the image analysis. All authors contributed to a critical discussion of the data. Kaushikaram Subramanian, Benjamin Seelbinder and Moritz Kreysing wrote manuscript. Authors Kaushikaram Subramanian, Heike Petzold and Benjamin Seelbinder contributed equally.

## DATA AVAILABILITY STATEMENT

The data that support the findings of this study are available from the corresponding author upon reasonable request.

## ORCID

Kaushikaram Subramanian  <https://orcid.org/0000-0002-9050-5672>

## REFERENCES

- [1] D. Toomre, J. Bewersdorf, *Annu. Rev. Cell Dev. Biol.* **2010**, 26, 285.
- [2] S. J. Sahl, S. W. Hell, S. Jakobs, *Nat. Rev. Mol. Cell Biol.* **2017**, 18, 685.
- [3] J. Huisken, D. Y. R. Stainier, *Development* **2009**, 136, 1963.
- [4] M. A. Lancaster, J. A. Knoblich, *Science* **2014**, 345, 1247125.
- [5] A. G. Botton, *Diabetes, Obes. Metab.* **2016**, 18, 33.
- [6] N. Prior, P. Inacio, M. Huch Ortega, *Gut* **2019**, 68, 2228.
- [7] J. F. Dekkers, M. Alieva, L. M. Wellens, H. C. R. Ariese, P. R. Jamieson, A. M. Vonk, G. D. Amatngalim, H. Hu, K. C. Oost, H. J. G. Snippert, J. M. Beekman, E. J. Wehrens, J. E. Visvader, H. Clevers, A. C. Rios, *Nat. Protoc.* **2019**, 14, 1756.
- [8] H. C. van de Hulst, *Light Scattering by Small Particles*, Courier Corporation, Mineola, NY, **1981**.
- [9] S. Johnsen, *The Optics of Life*, Princeton University Press, Princeton, NJ, **2012**.
- [10] S. L. Jacques, *Phys. Med. Biol.* **2013**, 58, R37.
- [11] R. Samatham, S. L. Jacques, in *Biomedical Applications of Light Scattering III* (Eds: A. Wax, V. Backman), McGraw-Hill, New York, **2010**.
- [12] J. L. Cox, R. A. Farrell, R. W. Hart, M. E. Langham, *J. Physiol.* **1970**, 210, 601.
- [13] K. M. Meek, C. Knupp, *Prog. Retin. Eye Res.* **2015**, 49, 1.
- [14] K. Subramanian, M. Weigert, O. Borsch, H. Petzold, A. Garcia-Ulloa, E. W. Myers, M. Ader, I. Solovei, M. Kreysing, *eLife* **2019**, 8. <https://doi.org/10.7554/eLife.49542>.
- [15] I. Solovei, M. Kreysing, C. Lanctôt, S. Kösem, L. Peichl, T. Cremer, J. Guck, B. Joffe, *Cell* **2009**, 137, 356.
- [16] J. E. Dowling, *The Retina*, Harvard University Press, Cambridge, Massachusetts, **1987**.
- [17] A. Yoshida, M. Motoyama, A. Kosaku, K. Miyamoto, *Zool. Sci.* **1997**, 14, 737.
- [18] I. R. Hooper, P. Vukusic, R. J. Wootton, *Opt. Express* **2006**, 14, 4891.
- [19] G. Chapman, *Experientia* **1976**, 32, 123.
- [20] R. H. Siddique, G. Gomard, H. Hölscher, *Nat. Commun.* **2015**, 6, 1.
- [21] S. Johnsen, *Biol. Bull.* **2001**, 201, 301.
- [22] D. S. Richardson, J. W. Lichtman, *Cell* **2015**, 162, 246.
- [23] M. Kinnunen, A. V. Bykov, J. Tuorila, T. Haapalainen, A. V. Karmenyan, V. V. Tuchin, *J. Biomed. Opt.* **2014**, 19, 071409.
- [24] M. Delaye, A. Tardieu, *Nature* **1983**, 302, 415.

- [25] L. Takemoto, C. M. Sorensen, *Exp. Eye Res.* **2008**, *87*, 496.
- [26] M. A. Wride, *Philos. Trans. R. Soc. Lond. B Biol. Sci.* **2011**, *366*, 1219.
- [27] L. G. Henyey, J. L. Greenstein, *Astrophys. J.* **1941**, *93*, 70.
- [28] M. Born, E. Wolf, A. B. Bhatia, P. C. Clemmow, D. Gabor, A. R. Stokes, A. M. Taylor, P. A. Wayman, W. L. Wilcock. Principles of Optics: Electromagnetic Theory of Propagation, Interference and Diffraction of Light, 7th ed., Cambridge University Press, Cambridge, **1999**.
- [29] D. Watson, N. Hagen, J. Diver, P. Marchand, M. Chachisvilis, *Biophys. J.* **2004**, *87*, 1298.
- [30] A. G. Hoekstra, A. V. Chernyshev, K. A. Semyanov, M. A. Yurkin, P. A. Tarasov, V. P. Maltsev, *Appl. Optics* **2005**, *44*, 5249.
- [31] Y. Kosugi, R. Sato, S. Genka, N. Shitara, K. Takakura, *Cytometry* **1988**, *9*, 405.
- [32] H. M. Shapiro, *Practical Flow Cytometry*, John Wiley & Sons, Hoboken, NJ, **2005**.
- [33] J. R. Mourant, M. Canpolat, C. Brocker, O. Esponda-Ramos, T. M. Johnson, A. Matanock, K. Stetter, J. P. Freyer, *J. Biomed. Opt.* **2000**, *5*, 131.
- [34] R. Drezek, M. Guillaud, T. Collier, I. Boiko, A. Malpica, C. Macaulay, M. Follen, R. Richards-Kortum, *J. Biomed. Opt.* **2003**, *8*, 7.
- [35] O. C. Marina, C. K. Sanders, J. R. Mourant, *Biomed. Opt. Express* **2012**, *3*, 296.
- [36] T. Iskratsch, H. Wolfenson, M. P. Sheetz, *Nat. Rev. Mol. Cell Biol.* **2014**, *15*, 825.
- [37] Y. Li, D. Lovett, Q. Zhang, S. Neelam, R. A. Kuchibhotla, R. Zhu, G. G. Gundersen, T. P. Lele, R. B. Dickinson, *Biophys. J.* **2015**, *109*, 670.
- [38] B. Seelbinder, A. K. Scott, I. Nelson, S. E. Schneider, K. Calahan, C. P. Neu, *Biophys. J.* **2020**, *118*, 2627.
- [39] C. C. DuFort, M. J. Paszek, V. M. Weaver, *Nat. Rev. Mol. Cell Biol.* **2011**, *12*, 308.
- [40] R. Zaidel-Bar, *J. Cell Biol.* **2009**, *186*, 317.
- [41] C. Salameh, F. Salviat, E. Bessot, M. Lama, J.-M. Chassot, E. Moulongui, Y. Wang, M. Robin, A. Bardouil, M. Selmane, F. Artzner, A. Marcellan, C. Sanchez, M.-M. Giraud-Guille, M. Faustini, R. Carminati, N. Nassif, *Proc. Natl. Acad. Sci. U. S. A.* **2020**, *73*, 202001178.
- [42] C. E. Rommel, C. Dierker, L. Schmidt, S. Przibilla, G. von Bally, B. Kemper, J. Schnekenburger, *J. Biomed. Opt.* **2010**, *15*, 041509.
- [43] W. Choi, C. Fang-Yen, K. Badizadegan, S. Oh, N. Lue, R. R. Dasari, M. S. Feld, *Nat. Methods* **2007**, *4*, 717.
- [44] M. Schürmann, J. Scholze, P. Müller, J. Guck, C. J. Chan, *J. Biophotonics* **2016**, *9*, 1068.
- [45] S. Johnsen, E. A. Widder, *J. Theor. Biol.* **1999**, *199*, 181.
- [46] G. C. Brown, *J. Theor. Biol.* **1991**, *153*, 195.
- [47] D. E. Atkinson, *Curr. Top. Cell. Regul.* **1969**, *1*, 29.
- [48] R. Barrangou, J. A. Doudna, *Nat. Biotechnol.* **2016**, *34*, 933.
- [49] Y. Wakamatsu, S. Pristiyazhnyuk, M. Kinoshita, M. Tanaka, K. Ozato, *Proc. Natl. Acad. Sci. U.S. A.* **2001**, *98*, 10046.
- [50] K. Chung, K. Deisseroth, *Nat. Methods* **2013**, *10*, 508.

## SUPPORTING INFORMATION

Additional supporting information may be found online in the Supporting Information section at the end of this article.

**How to cite this article:** Subramanian K, Petzold H, Seelbinder B, Hersemann L, Nüsslein I, Kreysing M. Optical plasticity of mammalian cells. *J. Biophotonics*. 2021;14:e202000457. <https://doi.org/10.1002/jbio.202000457>